

Potentials and Limitations of MEO SAR

Jalal Matar, DLR, Jalal.Matar@dlr.de, Germany

Paco López-Dekker, DLR, Francisco.LopezDekker@dlr.de, Germany

Gerhard Krieger, DLR, Gerhard.Krieger@dlr.de, Germany

Abstract

This paper discusses various aspects of Synthetic Aperture Radar (SAR) missions in Medium Earth Orbits (MEO). It covers the design of suitable orbits and their corresponding coverage, with emphasis on repeat ones. Furthermore, it analyses the changes in SAR performance as altitude increases, while addressing the potentials and limitations of high orbits. Throughout the paper one interesting orbit, repeating its ground track every 3 days and providing near-global coverage, is studied.

1 Introduction

Natural disasters, like the recent earthquake that hit Nepal in April 2015, occur every now and then causing huge losses in lives and properties. Unfortunately, such disasters cannot be prevented, however, they may be anticipated and dealt with suitably once they occur.

SAR systems play an important role in creating risk assessment models for areas that are most likely to face natural disasters (e.g. Earthquakes, Volcanic eruptions, tsunamis, etc.); besides, crisis management benefits from the data provided by these systems, as a way to assess the distribution of the destruction and define rescue paths. Up till now geoinformation is still required to coordinate and assist emergency measures once such disasters occur.

Current Low Earth Orbit (LEO) SAR systems do provide us with these data, but the time required to get the data depends on when will the satellite pass over the area. Increasing orbital altitude towards MEO heights provides advantages with respect to spatial coverage, global temporal revisit times and communications infrastructure. This allows us to have the same coverage as in LEO within few days. MEO is capable of providing daily regional coverage and semi-global coverage within 3 days, using one satellite only.

2 Medium Earth Orbits (MEO)

Medium Earth Orbits occupy an altitude window from 2000 km to 35786 km. They are currently being used by communication and global positioning satellites, e.g., GPS(20200 km), GLONASS(19100 km) and Galileo(23222 km).

2.1 Repeat-Ground-Track (RGT) MEO

A repeat orbit repeats its ground track after a certain time interval. Such orbits are of great interest for Earth-observation missions, especially SAR missions, because they allow interferometric and change detection measurements for a large number of applications. It also means

that observations and measurements can be scheduled on a routine basis.

Repeat orbits are generally described by two parameters: N_d representing the number of days after which the orbit repeats, and N_p representing the number of revolutions completed in the time interval N_d . These two parameters are related by the period of repetition $T_r = N_p T_\Omega = N_d T_{\Omega G}$, where T_Ω is the nodal period and $T_{\Omega G}$ is the Greenwich's nodal period [8].

Various methods and methodologies have been developed through the years in order to predict Repeat-Ground-Track orbits (RGT-orbits). In our current work, the Epicyclic motion Repeat ground track Orbit (ERO) method, based on the epicyclic motion theory by Aorpmi and Palmer [1], was adopted because its whole concept is based on two orbital elements (inclination i and the right ascension of ascending node Ω) and two polar elements (radius r and argument of latitude u). It also includes the geopotential terms: J_2 , J_4 first order and J_2 second order. The eccentricity e is introduced to this method by applying a Simplified Repeat Ground track (SRG) refinement to the preliminary ERO solutions [3].

Using the method above, we can notice the existence of many repeat orbits with different repeat cycles. The next step is to find the orbit which will provide us with the needed coverage according to our specific applications.

Orbital Day

A repeat orbit repeats its ground track in N_d orbital days, after performing N_p revolutions around the Earth. The orbital day here is neither a sidereal day nor a normal 24 hours day, but is defined in the same way as the nodal period of Greenwich:

$$D = \frac{2\pi}{\omega_e - \dot{\Omega}}, \quad (1)$$

where ω_e is the angular velocity of Earth and $\dot{\Omega}$ is the orbital precession rate. If $D = 86164.0905 \text{ sec} \approx 23.934 \text{ hours}$, then the day is a sidereal day. If $D = 86400 \text{ sec} = 24 \text{ hours}$, then the day is a solar day or civil day. However, for an orbital plane the precession rate $\dot{\Omega}$

varies, depending on the orbital semi-major axis a , eccentricity e and inclination i . A more accurate model of the nodal regression can be found in [7].

2.2 Sun-synchronicity in MEO

All objects orbiting in a sun-synchronous orbit appear in the same position with respect to the sun. Thus a dawn-dusk sun-synchronous orbit experiences near continuous illumination throughout the whole year. Radar Satellites rely heavily on solar power in order to charge their on-board batteries, hence benefiting from such energy efficient orbits. The existence of these orbits require the precession rate $\dot{\Omega}$ of the orbit to be equal to the mean motion of the Earth around the sun

$$\dot{\Omega} = -1.5J_2 \sqrt{\frac{\mu}{a^3}} \frac{R_e^2}{a^2(1-e^2)^2} \cos(i) = 360^\circ/y, \quad (2)$$

where $J_2 = 0.00108263$ is the second zonal coefficient, μ is the Earth's gravitational constant, R_e is the Earth's radius and y is one year [6].

In (2), we notice that the only three variables are a , e and i , whereas the rest of the parameters are constants. Thus, a sun-synchronous orbit can be found for any combination of these three variables fulfilling (2). The required inclination for a sun-synchronous orbit is then

$$i = \cos^{-1} \left(-\frac{\dot{\Omega} a^2 (1-e^2)^2}{1.5J_2 \sqrt{\frac{\mu}{a^3}} R_e^2} \right). \quad (3)$$

The cosine function above imposes a restriction on the maximum altitude of sun-synchronous orbits, where

$$a \leq \sqrt[7]{\frac{1.5^2 J_2^2 R_e^4 \mu}{\dot{\Omega}^2 (1-e^2)^4}} \approx 12352 \text{ km}. \quad (4)$$

Sun-synchronous orbits cease to exist at orbital altitudes beyond 5974 km ($e = 0$). However, at higher MEO altitudes the satellite is in the Earth's shadow for shorter periods. Hence, non sun-synchronous energy efficient orbits can still be found by spending a bit more effort on power planning.

3 Coverage

Coverage is a key element in mission design, especially in those related to monitoring Earth's lithosphere. When talking about coverage, we must differentiate between two different aspects: *footprint* and *access area* [5].

3.1 Footprint

The footprint represents the actual area an instrument can see at any moment. It has a width, known as the swath width sw , which depends on the beamwidth of the radar antenna θ_{el} and the near incident angle θ_{inc1} :

$$sw = R_e \cdot (\theta_{inc2} - \theta_{inc1} - \theta_{el}), \quad (5)$$

where

$$\theta_{inc2} = \arcsin \left(\sin(\theta_{lk1} + \theta_{el}) \cdot \frac{R_e + h_{orb}}{R_e} \right) \quad (6)$$

is the far incident angle, h_{orb} is the orbital altitude and θ_{lk1} is the near look angle, which can be derived from θ_{inc1} according to the general look-incidence equation

$$\theta_{lk,n} = \sin^{-1} \left(\frac{R_e}{R_e + h_{orb}} \sin(\theta_{inc,n}) \right). \quad (7)$$

3.2 Access Area

The access area is the total area on ground that can be potentially seen by the spacecraft, based on its geometrical location in space. It can be calculated according to the range of incident angles at which the radar antenna can transmit and still receive useful data. Hence, the full access swath can be defined as:

$$sw_{full} = 2R_e \sin^{-1} \left(\frac{h_{orb} \cdot (\tan(\theta_{lk2}) - \tan(\theta_{lk1}))}{2R_e} \right), \quad (8)$$

where θ_{lk2} and θ_{lk1} represent the far and near range radar look angles, respectively, and are directly related to the incident angles through (7).

3.3 Global Coverage

Global coverage is achieved, if the swath of a certain satellite, or constellation of satellites, is able to cover the whole Earth within a certain period of time.

To get a rough approximation regarding the required swath width for a certain repeat orbit, we consider the number of revolutions N_p for an orbit to repeat, and we take the best case scenario where all swaths are packed next to each other, in a way that they cover the whole equator. Then, the required swath width is

$$sw_{req} > \frac{2\pi R_e}{N_p} \cos(i) \cdot \frac{1}{2}. \quad (9)$$

The factor $\frac{1}{2}$ is due to the fact that each revolution contains two swaths: ascending and descending. However, these swaths often cross and the $\frac{1}{2}$ factor approaches 1. Hence, sw_{req} is the lower bound for the actual swath search.

By applying the above search algorithm to the RGT MEO of section 2.1, the percentage coverage of each orbit is calculated. One of the fastest repeat orbits providing near-global coverage at an altitude of 6901 km is the non sun-synchronous "3/17 RGT orbit" which repeats its ground track every 3 days, completing 17 revolutions. Table 1 below shows the parameters of this orbit and figure 1 shows its coverage map. Of course, there exist other adequate MEO repeat orbits, but this orbit is chosen as one sample of many which will be examined thoroughly in future works.

Parameter	Value
Days to repeat N_d	3 orbital days
Number of revolutions for repeat N_p	17 revs
Inclination i - Eccentricity e	130 deg - 0
Right ascension of the ascending node Ω	359 deg
Argument of latitude u	120 deg
Incident angles θ_{inc}	20 to 47 deg

Table 1: 3/17 RGT Near-Global Coverage

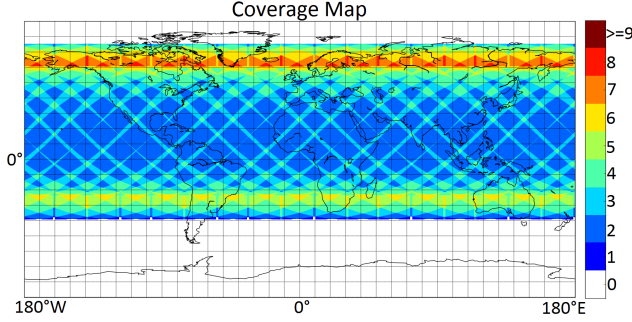


Figure 1: 3/17 Near-Global Coverage (right looking)

3.4 Regional Coverage

When it comes to regional coverage, MEO is a very good candidate. Due to its high altitude and in turn wide swath, regional coverage of large areas can be achieved within one or a few days. For example, the orbit of Table 2 can achieve regional coverage of Europe within one day as shown in figure 2.

Parameter	Value
Days to repeat N_d	1 orbital day
Number of revolutions for repeat N_p	2 revs
Inclination i - Eccentricity e	65 deg - 0
Right ascension of the ascending node Ω	359 deg
Argument of latitude u	120 deg
Incident angles θ_{inc}	20 to 45 deg

Table 2: 1/2 RGT Regional Coverage (Europe)

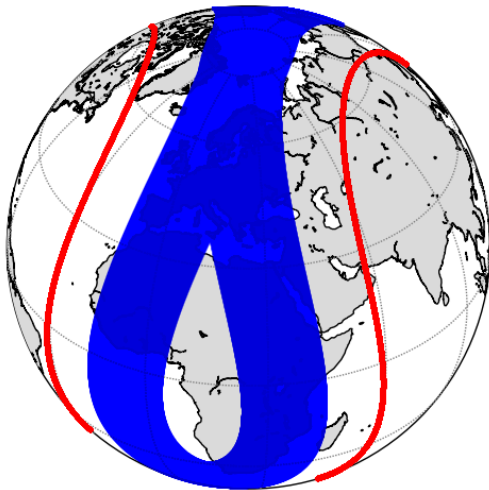


Figure 2: 1/2 RGT Regional Coverage (Europe)

4 Performance

4.1 Imaging Performance

SAR images can be characterized by their resolution: both in range (δ_{gr}) and azimuth (δ_{az}). The current resolution models found in the literature define these two parameters as follows [4]:

$$\delta_{gr} = \frac{c}{2\Delta f \sin \theta_{inc}} \quad (10)$$

where Δf is the bandwidth of the transmitted pulse, c is the speed of light and

$$\delta_{az} \approx L_{az}/2, \quad (11)$$

where L_{az} is the length of the SAR antenna.

The azimuthal resolution approximation δ_{az} works quite well for LEO orbits, where the satellite's trajectory is approximated by a straight line. However, when the orbital height increases, this assumption fails. One way to explain the difference is that at higher altitudes the natural steering of the radar antenna to always point towards a direction that is close to the Earth's center leads to an operation mode similar to that of a Spotlight mode [2].

The result of such a mode is a change in the azimuth resolution by a factor F_{az} , generated by the ratio of the ground track illuminated by the radar beam to the orbital path traveled by the satellite within the same time interval, leading to a significant improvement in the azimuth resolution. The general form for azimuthal resolution is then $\delta_{az} = \frac{L_{az}}{2} \cdot F_{az}$, where

$$F_{az} \approx \frac{R_e}{R_e + h_{sat}} \cos(\theta_{inc} - \theta_{lk}) < 1, \quad (12)$$

and h_{sat} represents the satellite's altitude.

4.2 Radiometric Performance (NESZ)

Noise Equivalent Sigma Zero (NESZ) is a very important sensitivity parameter in SAR systems. It is given by the value of the backscatter coefficient σ_0 corresponding to a signal-to-noise ratio of unity, and can be calculated as follows [4]:

$$NESZ = \frac{(4\pi)^2 R^3}{P_{avg} G_{TX} A_{eff}} \cdot \frac{2v_{sat}}{\lambda \delta_{gr}} \cdot L \cdot k_b \cdot T_{sys}, \quad (13)$$

where P_{avg} is the average transmit power, G_{TX} is the transmit gain, A_{eff} is the effective area of the receiving antenna, v_{sat} is the satellite velocity, λ is the signal's wavelength, R is the range to the target, k_b is the Boltzmann constant, L represents the system losses and T_{sys} is the system's noise temperature.

The NESZ changes with orbital altitude are shown in figure 3. The first two factors ΔR^3 and Δv_{sat} , have a direct impact on the NESZ. However, the impact of the change in the azimuth resolution by ΔF_{az} is not straight forward. If we think of it in terms of resolution, then it has no effect

on the NESZ. Nonetheless, if we want to have a fair comparison, we assume the same system requirements and characteristics (see table 3). This approach, whose results are shown in figure 3, exploits the azimuthal factor by varying δ_{gr} in accordance with δ_{az} , such that the total area of the resolution cell is preserved. The variation of δ_{gr} will in turn affect the system bandwidth. The last factor ΔG presenting the greatest advantage for higher orbits is related to the transmit gain

$$G_{TX} \approx \frac{16}{\sin \theta_{e1} \sin \theta_{az}}. \quad (14)$$

The gain here is considered to be reduced by the need to cover a larger swath than that provided by the antenna's beamwidth θ_{e1} (see section 3.1). This reduction can be explained by the need to distribute the total power on n sub-swaths, associated with Digital Beam Forming (DBF) on receive. Hence, we have a reduction in the gain by a factor n . The number of the required sub-swaths n is the ratio of the total beamwidth θ_{tot} required to cover the complete swath to that of the actual antenna θ_{e1} . Here comes the advantage of higher orbits, providing larger swaths for a given beamwidth and in turn reducing the number of required sub-swaths.

The negative sign in front of the factors $\Delta\delta_{gr}$, ΔG and later ΔA_{eff} is linked to their position in the denominator of (13).

Parameter	Value
Wavelength λ	0.2384 m
Antenna size $W_a \times L_a$	15 m \times 15 m
Required swath width sw_{req}	400 km
Incident angle θ_{inc}	30 deg

Table 3: General system characteristics (Approach 1)

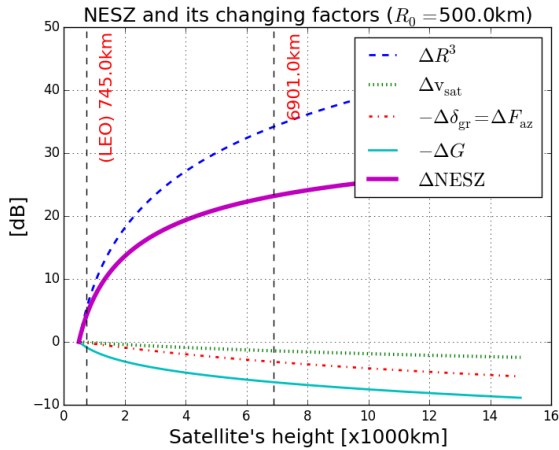


Figure 3: NESZ changing factors for different orbital heights (Approach 1) - $\Delta NESZ$ is the sum of all factors

Another approach is to fix all system parameters except for the antenna size (see table 4). The azimuthal factor can then be exploited by using bigger antennas at higher altitudes, in order to achieve the same azimuthal resolution δ_{az} . This leads to a direct increase in the transmit

gain G_{TX} and the effective area of the receiving antenna A_{eff} , hence, decreasing the difference in NESZ as shown in figure 4.

The minimum required antenna dimensions corresponding to this approach are plotted in figure 5. However, these dimensions should be modified in order to avoid range ambiguities within the covered swath.

Parameter	Value
Azimuth resolution δ_{az}	4 m
Wavelength λ	0.2384 m
Required swath width sw_{req}	200 km
Incident angle θ_{inc}	30 deg

Table 4: General system characteristics (Approach 2)

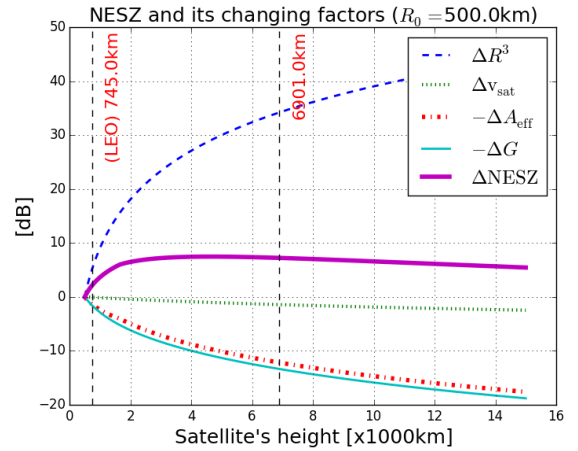


Figure 4: NESZ changing factors for different orbital heights (Approach 2) - $\Delta NESZ$ is the sum of all factors

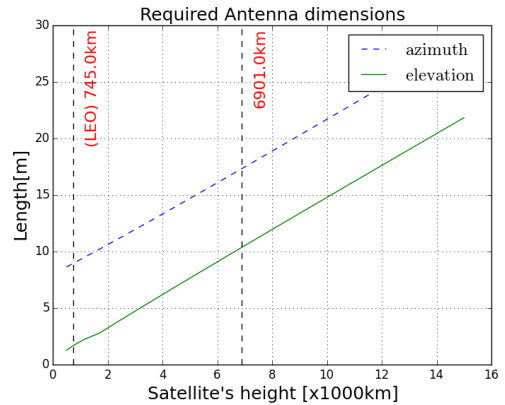


Figure 5: Required antenna dimensions (Approach 2)

Performance of the 3/17 RGT orbit

Figure 6 shows the approximate performance of the 3/17 RGT orbit described in table 1, with the system characteristics as in table 5. The first plot shows the NESZ, and is calculated according to (13). The second plot shows two Pulse Repetition Frequency (PRF) curves:

$$PRF_{min} = \frac{2v_{sat}}{L_{eff}}, \quad (15)$$

where L_{eff} is the antenna's effective length. PRF_{min} is the minimum required PRF at which the sampling of the azimuth information from each resolution cell can still be achieved as the platform advances, and

$$\text{PRF}_{\text{max}} = \frac{c}{2(R_2 - R_1)}, \quad (16)$$

where R_1 and R_2 are the near and far slant ranges, respectively. PRF_{max} is the maximum allowable PRF below which ambiguities caused by echoes from later pulses can still be avoided. The third plot shows the achievable resolutions δ_{gr} calculated according to (10) and δ_{az} which in this case is that obtained using a parabolic antenna and is approximated by:

$$\delta_{\text{az}} \approx \frac{D}{2} \cdot F_{\text{az}}, \quad (17)$$

where D is the antenna's diameter. The last plot shows the real sub-swath width calculated using (5) and the number of sub-swaths n needed to cover the total required swath sw_{req} .

Parameter	Value
Average transmit power P_{avg}	1 kW
System noise temperature T_{sys}	465 K
System losses L	3.6 dB
Wavelength λ	0.2384 m
System bandwidth Δf	50 MHz
Antenna type	Parabolic
Effective antenna area A_{eff}	180 m ²
Incident angles θ_{inc}	20 to 45 deg
Total required swath sw_{req}	1369 km

Table 5: 3/17 Mission: System characteristics

5 Conclusions

The preliminary studies done on MEO SAR so far show a great potential, especially with their short revisit times and bigger swath widths compared to LEO SAR systems. The difficulties related to MEO orbits are: reduced SNR, bigger antenna sizes, more power planning requirements (for orbits higher than sun-synchronous limit) and radiation issues which will be addressed in future investigations.

References

- [1] M. Aorpimai and P.L. Palmer. Repeat-groundtrack orbit acquisition and maintenance for earth-observation satellites. *Journal of guidance, control, and dynamics*, 30(3):654–659, 2007.
- [2] D.P. Belcher and C.J. Baker. Hybrid strip-map/spotlight sar. In *Radar and Microwave Imaging, IEE Colloquium on*, pages 2–1. IET, 1994.
- [3] S.K. Collins and P.J. Cefola. Computationally efficient modelling for long term prediction of global positioning system orbits. *Journal of the Astronautical Sciences*, 26:293–314, 1978.

- [4] J.C. Curlander and R.N. McDonough. *Synthetic Aperture Radar Systems and Signal Processing*. New York: John Wiley & Sons, 1991.
- [5] W.J. Larson and J.R. Wertz. *Space Mission Analysis and Design*, volume 8. Microcosm Press, 2007.
- [6] O. Montenbruck and E. Gill. *Satellite orbits: models, methods and applications*. Springer Science & Business Media, 2012.
- [7] D.A. Vallado. *Fundamentals of astrodynamics and applications*, volume 12. Springer Science & Business Media, 2001.
- [8] Bruccoleri C. Wilkins, M.P. and D. Mortari. Constellation design using flower constellations. *Paper AAS*, pages 04–208, 2004.

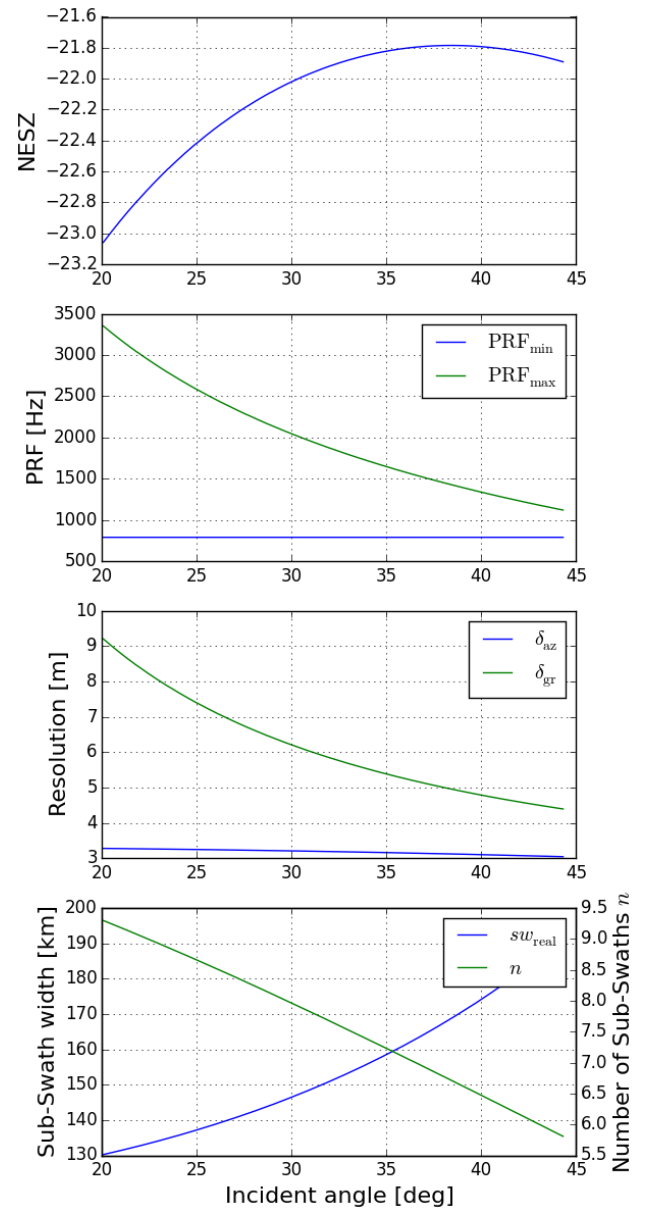


Figure 6: Performance of a 3/17 RGT orbit